Agricultural and Forest Meteorology 256–257 (2018) 75–83

Contents lists available at ScienceDirect

Agricultural and Forest Meteorology

journal homepage: www.elsevier.com/locate/agrformet

Spatio-temporal variation of potential evapotranspiration and climatic drivers in the Jing-Jin-Ji region, North China

Jingyan Han[a,b], Jianhua Wang[a], Yong Zhao[a,*], Qingming Wang[a], Bing Zhang[c,*], Haihong Li[a], Jiaqi Zhai[a]

[a] State Key Laboratory of Simulation and Regulation of Water Cycle in River Basin, China Institute of Water Resources and Hydropower Research, Beijing, 100038, China
[b] Department of Hydraulic Engineering, Tsinghua University, Beijing, 100084, China
[c] Tianjin Key Laboratory of Water Resources and Environment, Tianjin Normal University, 300387, Tianjin, China

ARTICLE INFO

Keywords:
Potential evapotranspiration
Climatic parameters
Shift point
Dominant factors
Jing-Jin-Ji region

ABSTRACT

Potential evapotranspiration (ET_0) is a key component of the water cycle and a main factor to water resources assessment. Analysis of variation in ET_0 is significant in understanding the climate change and agricultural water management; It is affected by multiple climatic factors, including air temperature, relative humidity, wind speed, and sunshine duration. To understand the variations of ET_0 in the Jing-Jin-Ji region (Beijing Municipality, Tianjin Municipality, and Hebei Province), values of ET_0 and other climatic parameters at 22 national meteorological stations from 1961 to 2015 were analyzed. Cramer's test showed a shift point in the ET_0 data at approximately 1991. Annual ET_0 decreased from 1961 through 1991 at a rate of −20.95 mm per decade, but annual ET_0 increased at a rate of 7.40 mm per decade from 1992 to 2015. Partial correlation analysis and multiple linear regression methods were used to determine the dominant climatic driving factors for ET_0, and to reveal the causes of change in ET_0. From 1961 to 1991, the decrease of wind speed and sunshine duration offset the effect of increased air temperature, leading to reduced ET_0. However, from 1992 to 2015, average air temperature was the most dominant factor contributing to the increase in ET_0. Increased of air temperature and wind speed, and decreased relative humidity caused an increase in ET_0. This change in ET_0 could impact hydrological cycle and agriculture irrigation management in the Jing-Jin-Ji region.

1. Introduction

Climate change has enormous environmental and socioeconomic implications. Many global issues potentially affected by climate change, such as food security, biodiversity loss and water scarcity, are affected by temperature, potential evapotranspiration, solar radiation and other factors together (Walther et al., 2002; Christensen et al., 2004; Zhao et al., 2014; Xu et al., 2017). Evapotranspiration, the only connection linking the water balance and land surface energy balance, is considered as a significant indicator for climate change and the water cycle (Tao et al., 2015). Due to lack of the observed evapotranspiration data, potential evapotranspiration is generally used to estimate the actual evapotranspiration, and is defined as the combined evaporation and transpiration by growing vegetation with access to an unlimited supply of water. ET_0 is influenced by incoming solar radiation, which provides the energy required to evaporate water, and also by wind, humidity and temperature (King et al., 2015). Trends in ET_0 directly affect regional and global water resources as part of the changing climate; analyzing trends in ET_0 can provide considerable insights into current climate change and its impact on water resources (Nam et al., 2015; Li et al., 2017). ET_0 is a main focus on water resource assessment, and also a foundation for the calculation of crop water requirements (Ma et al., 2012). Thus, the variation of ET_0 has been widely applied as valuable reference to assess agricultural water requirements, hydrological cycles, and ecological changes (Ning et al., 2016).

As the global climate becomes warmer and warmer, it is generally expected that the air will become drier. Evaporation from terrestrial water bodies will increase (Roderick and Farquhar, 2002). However, even as increasing air temperature has been observed over the last few decades, the pan evaporation or ET_0 has shown a steady downward trend; this is known as the 'evaporation paradox' phenomenon (Peterson et al., 1995). Decreased pan evaporation has been found in many locations, such as Italy, Australia, and New Zealand (Moonen et al. 2002; Roderick and Farquhar, 2005; Tabari and Marofi, 2010). Decreasing ET_0 has also been observed in the Haihe River basin (Ma et al., 2012), southwestern China (Li et al., 2014), northwest China (Xu

* Corresponding authors.
E-mail addresses: zhaoyong@iwhr.com (Y. Zhao), zhangbing@tjnu.edu.cn (B. Zhang).

https://doi.org/10.1016/j.agrformet.2018.03.002
Received 14 August 2017; Received in revised form 25 February 2018; Accepted 4 March 2018
Available online 20 March 2018
0168-1923/ © 2018 Elsevier B.V. All rights reserved.

et al., 2015), the Tibetan Platea (Zhang et al., 2007), the Loess Plateau (Ning et al., 2016) and many other regions of China (Tang et al., 2011; Ma et al., 2012; Zhu et al., 2012), but in recent years, increased pan evaporation or ET_0 has been identified in data since the 1980s in China. Cong et al. (2009) found that annual pan evaporation in China decreased from 1956 to 1985, related to decreasing daily maximum air temperature and wind speed. However, they also found that pan evaporation has increased since 1986, mainly due to an increasing vapor pressure deficit. Liu and Zhang (2013) investigated the ET_0 trends in the Northwest China from 1960 to 2010. ET_0 decreased from 1960 to 1993 mainly related to decreasing trends in wind speed, although it began to increase in 1994, mainly due to the increasing air temperature and wind speed. As changes in ET_0 differ greatly in different regions, it is essential to conduct regional research.

The Jing-Jin-Ji region (Beijing Municipality, Tianjin Municipality and Hebei Province), one of the three large regional economic communities in China, is located in semi-humid and semi-arid areas. Water resources are limited, but water demands have increased dramatically in this region, and there is a sharp conflict between urban growth and limited water resources (Dong et al., 2008). This region therefore has a large net water deficiency and faces a severe water shortage crisis. Agricultural irrigation is the largest water-consuming sector; data from 2003 to 2013 show that more than 70% of the supplied water in Hebei Province was consumed by agriculture. Agricultural water consumption accounted for 55% of the total water consumption in Tianjin Municipality, and approximately 33% of the consumption in Beijing Municipality (Fan et al., 2016). The rapid urbanization and economic development divert water from the agricultural sector to industrial and other sectors (Zhu et al., 2015), and agricultural water security and food security therefore face enormous pressure in the Jing-Jin-Ji region. Although water capacity in the Jing-Jin-Ji region may be improved after the South to North Water Transfer Project, the living standard might not to be improved because of the increasing population (Feng and Liu, 2006). ET_0 is the key component of water cycle, used for assessment of water deficiencies (Huang et al., 2014). Consequently, the analysis of ET_0 is an important indicator for understanding climate change, and also as a basis to improve water resource management.

The objectives of this study are: (1) to explore the spatio-temporal characteristics of ET_0 and climatic variables in the Jing-Jin-Ji region; (2) to identify the dominant climatic driving factors of ET_0; and (3) to reveal the reasons for changing ET_0 in the Jing-Jin-Ji region. The conclusions will improve the understanding of climate change, and provide valuable reference for regional water resources management and agriculture development.

2. Materials and methods

2.1. Study area

The Jing-Jin-Ji region (26°02′N–42°38′N, 113°25′–119°51′E) is part of the Haihe River basin, and is located in the northern part of the North China Plain (Fig. 1). The area consists of Beijing municipality, Tianjin municipality, and Hebei province, and has a total area of 213,600 km^2. Beijing is the capital city of China and has an area of 16,300 km^2. Tianjin is a municipality direct under the Central Government, as well as an expanding city with an area of 11,700 km^2. The area of Hebei province containing 11 major cities is 185,600 km^2 (Dong et al., 2008). There is a serious shortage of water resources in the region and a tremendous conflict between water supply and demand. This has resulted in severe environmental problems, including degradation of rivers and lakes, water pollution and land-surface subsidence due to over exploitation of groundwater (Xia et al., 2003).

2.2. Data source

We selected 22 meteorological stations in the Jing-Jin-Ji region for analysis of climatic parameters (Fig. 1). The climatic data from 1961 to 2015, including daily average air temperature (T_{mean}), minimum air temperature (T_{min}), maximum air temperature (T_{max}), relative humidity (RH), sunshine duration (SD), and wind speed (U_2), were downloaded from the National Climate Center, China Meteorological Administration (CMA) (http://data.cma.cn). These datasets are available and have been processed with quality control (Table 1).

2.3. Analytical methods

2.3.1. Calculation of ET_0

The Food and Agriculture Organization (FAO)56 Penman-Monteith (PM) model has been widely applied to calculate ET_0, and ET_0 at the 22 observation stations was calculated as:

$$ET_0 = \frac{0.408\Delta(R_n - G) + \gamma(900/(T_{mean} + 273))U_2 \cdot (e_s - e_a)}{\Delta + \gamma(1 + 0.34U_2)} \quad (1)$$

where ET_0 is the daily reference ET rate (mm day^{-1}), R_n is the net radiation at the ground surface (MJ m^{-2} day^{-1}), G is the soil heat flux density (MJ m^{-2} day^{-1}), T_{mean} is the mean daily air temperature at 2 m height (°C), U_2 is the wind speed at 2 m height (m s^{-1}), e_s is the saturation vapor pressure (kPa), e_a is the actual vapor pressure (kPa), $e_s - e_a$ is the saturation vapor pressure deficit (kPa), Δ is the slope of the vapor pressure curve (kPa °C^{-1}), and γ is the psychometric constant (kPa °C^{-1}).

Net radiation was estimated using the sunshine hours, maximum and minimum air temperatures data by following formulas:

$$R_n = R_{ns} - R_{nl} \quad (2)$$

$$R_{ns} = (1 - \alpha)R_s \quad (3)$$

$$R_s = \left(a_s + b_s\frac{n}{N}\right)R_a \quad (4)$$

$$R_a = \frac{24 \times 60}{\pi} \times G_{sc} \cdot d_r(\omega_s \sin\phi \sin\delta + \cos\phi \cos\delta \sin\omega_s) \quad (5)$$

where R_{ns} is the net short-wave radiation (MJ m^{-2} day^{-1}), α is the albedo coefficient, R_s is the incoming solar radiation(MJ m^{-2} day^{-1}), n is actual daily sunshine duration(h), which was measured in this study, N is the maximum possible duration of sunshine or daylight hours (h), R_a is the extraterrestrial radiation intensity (MJ m^{-2} day^{-1}), G_{sc} is solar constant (0.0820 MJ m^{-2} min^{-1}), d_r is inverse relative distance Earth-Sun, ω_s is sunset hour angle, ϕ is the station latitude, δ is solar declination. In this study, the coefficients $\alpha = 0.23$, $a_s = 0.25$ and $b_s = 0.50$ following by the recommendation of the FAO (Allen et al., 1998).

R_{nl} is net outgoing long-wave radiation(MJ m^{-2} day^{-1}), and was estimated as:

$$R_{nl} = \sigma\left(\frac{T_{max,K}^4 + T_{min,K}^4}{2}\right)(0.34 - 0.14\sqrt{e_a})(1.35\frac{R_s}{R_{so}} - 0.35) \quad (6)$$

$$R_{so} = (0.75 + 2 \times 10^{-5}z)R_s \quad (7)$$

$$e_a = \frac{RH}{100}e_s \quad (8)$$

$$e_s = \frac{0.6108\exp[\frac{17.27T_{max}}{T_{max} + 237.3}] + 0.6108\exp[\frac{17.27T_{min}}{T_{min} + 237.3}]}{2} \quad (9)$$

where σ is the StefanBoltzman constant (4.903×10^{-9} MJ K^{-4} m^{-2} day^{-1}), $T_{max,K}$ is maximum absolute temperature during the 24-h period (K), $T_{min,K}$ is minimum absolute temperature during the 24-h period (K), R_{so} is clear-sky radiation (MJ m^{-2} day^{-1}), z is station elevation above sea level (m).

Soil heat flux density was calculated as :

$$G = c_s(T_i - T_{i-1})\Delta z, \quad (10)$$

where c_s is the soil heat capacity (2.1 MJ m^{-3} °C^{-1}), Δz is effective

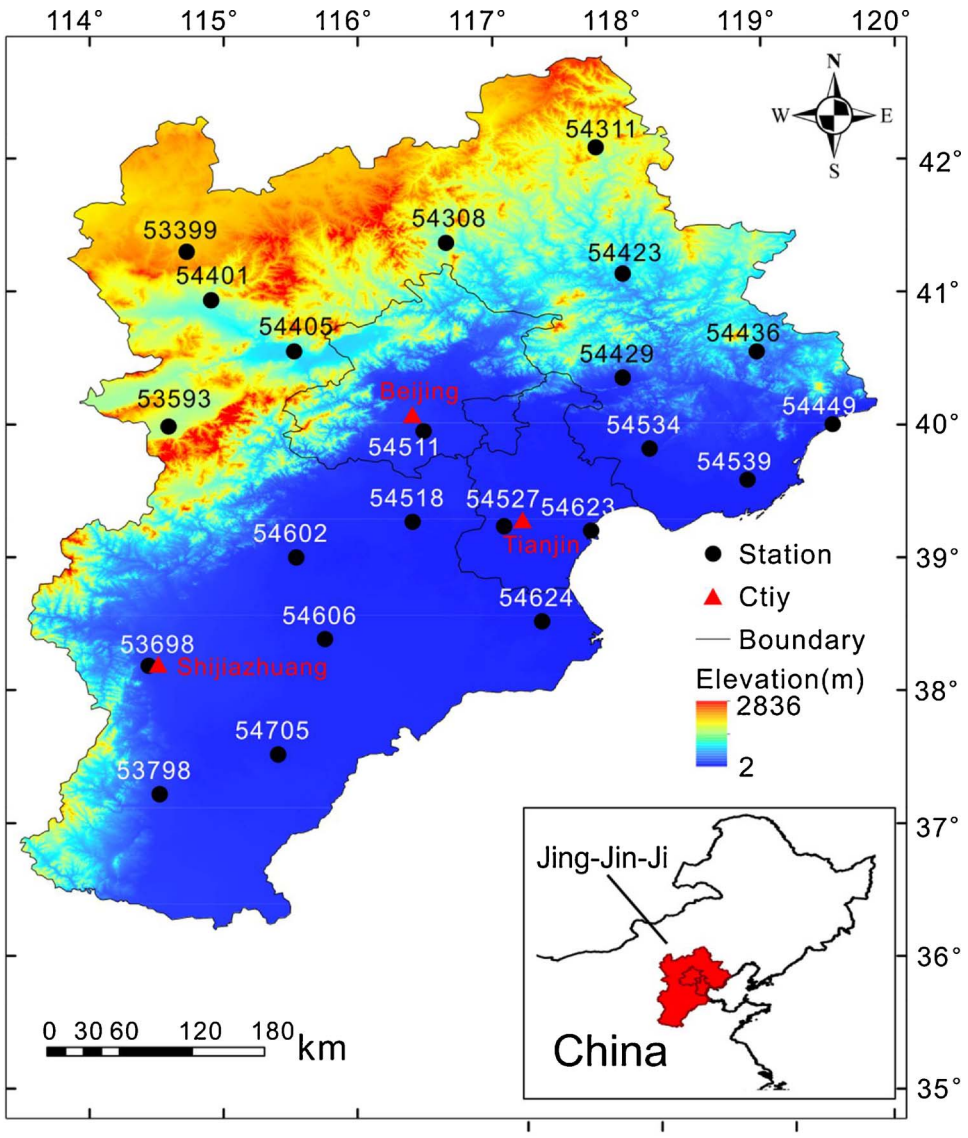

Fig. 1. Location of the study area and the distribution of meteorological stations.

Table 1
Basic information of the national meteorological stations in the study area.

Station code	Station name	Latitude (°N)	Longitude (°E)	Elevation (m)	Duration of data
54511	Beijing	39.80	116.47	31.3	1961–2015
54527	Tianjin	39.08	117.07	2.5	1961–2015
54623	Tanggu	39.05	117.72	4.8	1961–2015
53399	Zhangbei	41.15	114.70	1393.3	1961–2015
53593	Yuxian	39.83	114.57	909.5	1961–2015
53698	Shijiangzhuang	38.03	114.42	81.0	1961–2015
53798	Xingtai	37.07	114.50	77.3	1961–2015
54308	Fengning	41.22	116.63	661.2	1961–2015
54311	Weichang	41.93	117.75	842.8	1961–2015
54401	Zhangjiakou	40.78	114.88	724.2	1961–2015
54405	Huailai	40.40	115.50	536.8	1961–2015
54423	Chengde	40.98	117.95	385.9	1961–2015
54429	Zunhua	40.20	117.95	54.9	1961–2015
54436	Qinglong	40.40	118.95	227.5	1961–2015
54449	Qinhuangdao	39.85	119.52	2.4	1961–2015
54518	Langfang	39.12	116.38	9.0	1961–2015
54534	Tangshan	39.67	118.15	27.8	1961–2015
54539	Leting	39.43	118.88	10.5	1961–2015
54602	Baoding	38.85	115.52	17.2	1961–2015
54606	Raoyang	38.23	115.73	19.0	1961–2015
54624	Huanghua	38.37	117.35	6.6	1961–2015
54705	Nangong	37.37	115.38	27.4	1961–2015

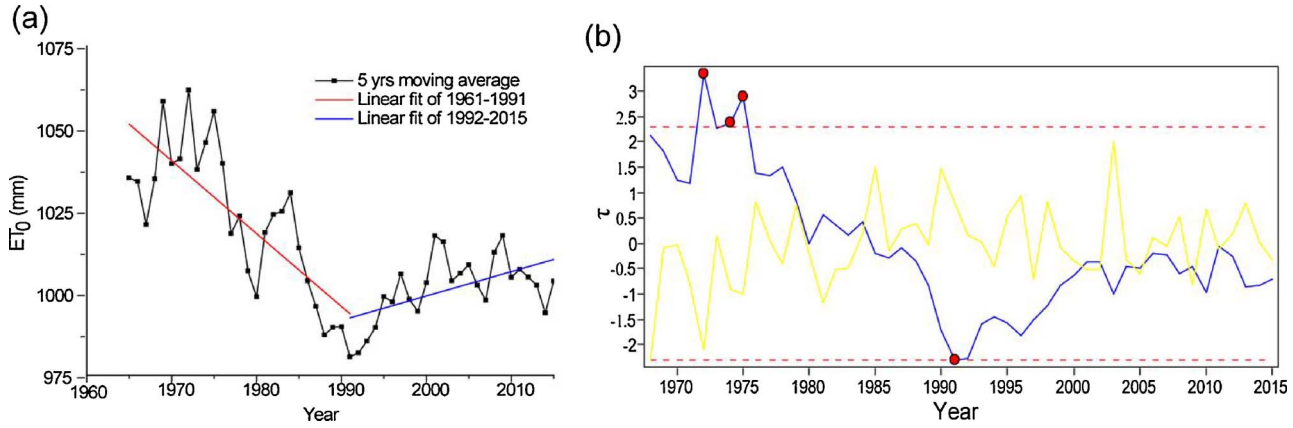

Fig. 2. Variation of annual ET_0 (a) and Cramer's test results for detecting change in annual ET_0 (b) in the Jing-Jin-Ji region from 1961 to 2015. The red points represent the years in which the mutation occurred in the ET_0 series. (For interpretation of the references to colour in this figure legend, the reader is referred to the web version of this article.)

soil depth (0.2 m), $T_i$is the average air temperature of the ith day, T_{i-1} is the average air temperature of the (i–1)th day.

After daily ET_0 values were calculated, they were transformed into ET_0 at an annual scale.

The Cramer test method is used in the study to detect the mutation of ET_0 series.

2.3.2. Mann–Kendall test for trend analysis

The Mann–Kendall (MK) test has been widely used for the analysis of hydrologic and meteorological trends (Tabari and Marofi, 2010; Wang et al., 2011; Zhang et al., 2015; Gao et al., 2017). The rank-based Mann–Kendall method is a common nonparametric method used to assess the significance of monotonic trends in hydro-meteorological time series. This test has the advantage of not assuming any distribution form for the data and has a similar power to its parametric competitors. Therefore, it is highly recommended for general use by the World Meteorological Organization. In the MK test, the statistical value S and the standardized test statistics Z are calculated as follows (Liu et al., 2014; Zhang et al., 2015; Lin et al., 2017) :

$$S = \sum_{i=1}^{n-1} \sum_{j=i+1}^{n} \operatorname{sgn}(x_j - x_i) \tag{11}$$

$$\operatorname{sgn}(x_j - x_i) = \begin{cases} 1 & if\ (x_j - x_i) > 0 \\ 0 & if\ (x_j - x_i) = 0 \\ -1 & if\ (x_j - x_i) < 0 \end{cases} \tag{12}$$

$$\sigma_s^2 = \frac{n(n-1)(2n+5) - \sum_{p=1}^{q} t_p(t_p-1)(2t_p+5)}{18} \tag{13}$$

$$z = \begin{cases} \frac{s-1}{\sigma^s} & if\ s > 0 \\ 0 & if\ s = 0 \\ \frac{s+1}{\sigma^s} & if\ s < 0 \end{cases} \tag{14}$$

where x_i and x_j are two generic sequential values of the variable, n is the length of the data set, q is the number of tied groups, and t_p is the number of data values in the pth group. The Z value is used to evaluate the statistical trend; a positive Z value represents an upward trend, while a negative Z value indicates a declining trend. For a two-tailed test at α level of significance, H_0 is rejected at the two-sided significant level of α if $|Z| > Z_{1-\alpha/2}$.

2.3.3. Partial correlation analysis

Partial correlation analysis was used to examine the relationships between ET_0 and the climatic driving factors. In this analysis, the relationship between two variables is determined while controlling the possible influences of all other factors. It can be inferred that the larger a partial correlation coefficient is, the more important that factor is for changes of ET_0. (Gao et al., 2006; Wang et al., 2011).

2.3.4. Multiple linear regression

Multiple linear regression analysis on meteorological factor series were performed to establish the multiple regression equations involving one or more independent variables, and can best predict the value of the dependent variable. The relative contributions were calculated using the following formulas (Li et al., 2014):

$$Y_S = aX_{1s} + bX_{2s} + cX_{3s} + \cdots, \tag{15}$$

$$n_1 = |a|/(|a| + |b| + |c| + \cdots), \tag{16}$$

where Y_s is the standardized value of ET_0, X_{1s}, X_{2s}, X_{3s}..are standardized values of the first meteorological factor, the second meteorological factor, the third meteorological factor, etc., a, b, c. are regression coefficients for the first meteorological factor, the second meteorological factor, the third meteorological factor, etc., and n_1 is the relative contribution of the variation of X_{1s} to the ET_0.

3. Results and discussion

3.1. Change in ET0 and climatic driving factors

Cramer's test is used in the study to detect the mutation of ET_0 series. Fig.2(a) shows the trends of annual ET_0 in the Jing-Jin-Ji region from 1961 to 2015. Fig. 2(b) shows the results of Cramer's test for detecting the mutation of annual ET_0 series. There were inflection points in 1972, 1974, 1975 and 1991. In the short term, the trend of ET_0 tend rises and then begins to decline in the 1970s, but because of the lack of data before 1961, it could not be determined whether the years 1972, 1974 and 1975 were real change points in the long-term series. However, the slope of the annual ET_0 series changed significantly in approximately 1991 across the entire period. Hence, the year 1991 is selected as a breaking point, and the study period from 1961 to 2015 is divided into two parts: a 31-year period from 1961 to 1991 and a 24-year period from 1992 to 2015. Annual ET_0 decreased significantly ($p < 0.01$) by −20.95 mm per decade before 1991, but increased significantly ($p < 0.05$) by 7.40 mm per decade after 1991 (Table 2). What causes this change of ET_0 after 1991? Because variation in ET_0 is results from the combined effect of climatic variables such as mean air temperature, relative humidity, sunshine duration and wind speed, the analysis of each climatic variable before and after 1991 is necessary. The inflection point of ET_0 is used as the basis of the division period, and this time point is applied in the analysis of other climatic variables, similar to the approach of Liu and Zhang (2013) and Zhang et al. (2013). The trends and Z-values of climate variables in two study

Table 2
Trends, Z-values from MK test of ET_0 and climate variables in Jing-Jin-Ji region from 1961 to 2015.

	Period	ET_0	T_{mean}	T_{max}	T_{min}	RH	SD	U_2
trend	1961–1991	−20.95**	0.20**	0.15*	0.39**	−0.48	−55.6**	−0.18**
	1992–2015	7.40*	0.10	0.08	0.16*	−1.17**	−96.6**	0.06**
Z-value	1961–1991	−3.68	3.42	2.27	4.52	−1.65	−5.31	−4.87
	1992–2015	2.43	1.40	1.12	2.06	−4.16	−5.75	3.176

Trend is the slope of linear regression between meteorological factors and year; The slope units of ET_0, *T, RH, SD,* U_2 are mm/decade, °C/decade, %/decade, h/decade, and m/s/decade, respectively;

* Significance levels of 0.05 ($P < 0.05$).

** Significance levels of 0.01 ($P < 0.01$).

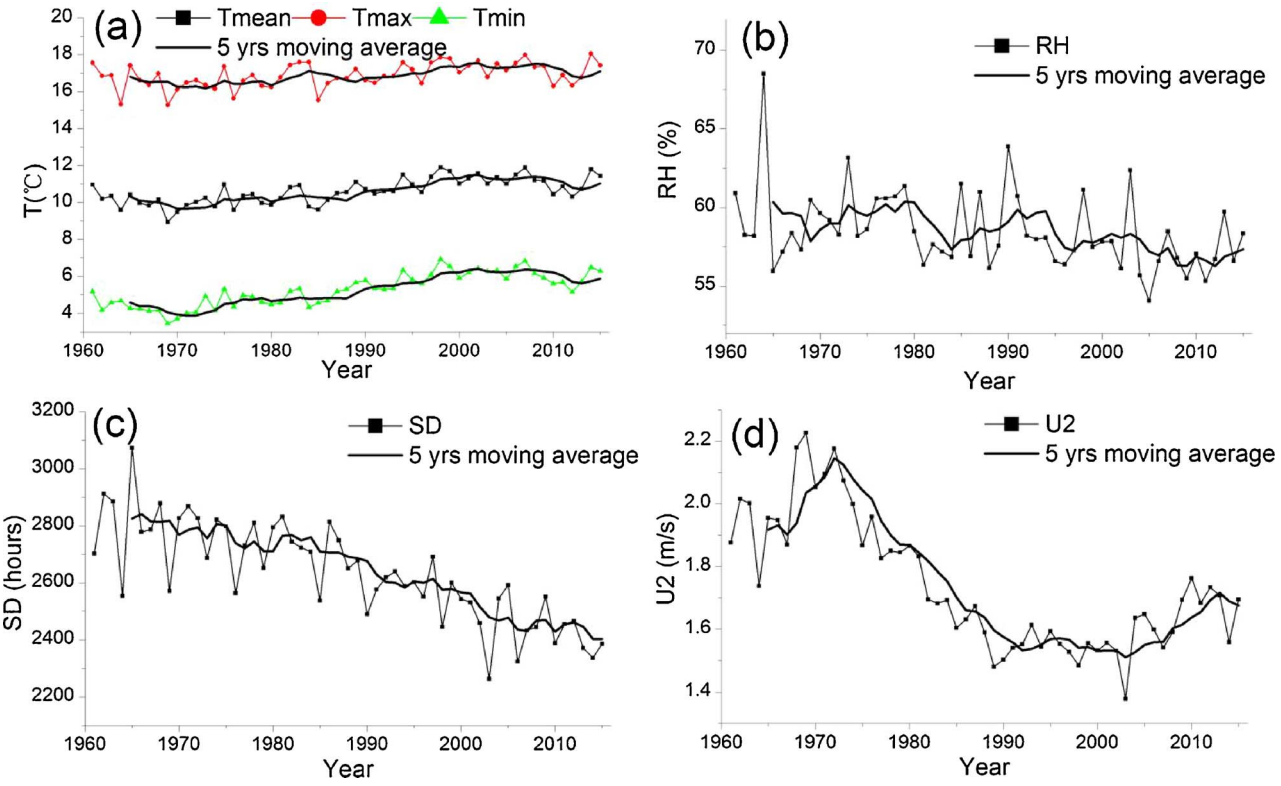

Fig. 3. Annual average and 5-year moving average air temperature,*T* (a), relative humidity, *RH* (b), sunshine duration, *SD* (c) and wind speed, U_2 (d) of the Jing-Jin-Ji region from 1961 to 2015.

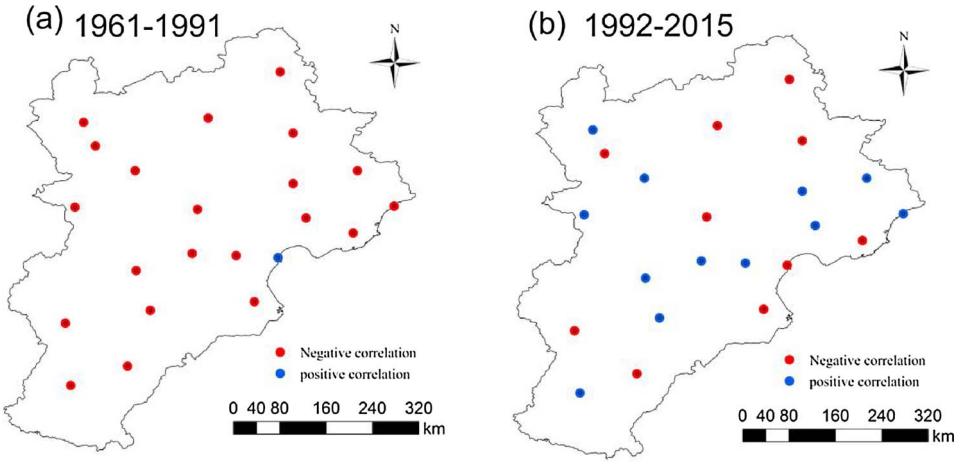

Fig. 4. Correlations between ET_0 and T_{mean} for the 22 meteorological stations (a) 1961–1991; (b) 1992–2015. Negative correlation indicates stations displaying evaporation paradox; positive correlation indicates no evaporation paradox phenomenon.

periods are listed in Table 2.

Table 1 and Fig.3 shows the trends of climate variables in the Jing-Jin-Ji region from 1961 to 2015. Before 1991, Annual mean air temperature, maximum air temperature, and minimum air temperature increased significantly ($p < 0.01$) at rates of 0.20 °C, 0.15 °C, and 0.39 °C per decade, respectively. After 1991, the upward trend was relatively weak, at rates of 0.10 °C, 0.08 °C, and 0.16 °C per decade, respectively. This indicates that the increasing amplitude of air temperature has declined. *RH* showed decreasing trends of −0.48% and −1.17% ($p < 0.01$) per decade before and after 1991, respectively. The downward trend was steeper during the period from 1992 to 2015 than during the previous 31 years. Annual *SD* decreased sharply during both periods, showing a significant ($p < 0.01$) declining trend with a reduction of −55.6 h per decade and −96.6 h per decade before and after 1991, respectively. U_2 decreased dramatically ($p < 0.01$) by −0.18 m/s per decade from 1961 to 1991, but a significant ($p < 0.01$) slight increasing trend was observed at a rate of 0.06 m/s per decade after 1991. These results show opposite trends of ET_0 and U_2 during the period 1992–2015 compared to the period 1961–1991. ET_0 decreased with increasing air temperature from 1961 to 1991, but it appears increasing trends with increasing air temperature after 1991.

Fig.4 shows the correlations between ET_0 and T_{mean} for the 22 meteorological stations before and after 1991. From 1961 to 1991, the evaporation paradox phenomenon was found at almost every station throughout the region; only 1 station (Tanggu) had an increasing trend of ET_0 with increasing temperature (Fig. 4a). However, quite a few stations changed significantly after 1991, and ET_0 trends may have started to reverse. The number of stations with positive correlations between ET_0 and temperature was much greater than during the pre-1991 period, accounting for 54% of the total stations (Fig. 4b). The analysis of the temperature and ET_0 trends demonstrated the existence of the evaporation paradox in the Jing-Jin-Ji region during the 1961–1991 period, but not from in 1992 to 2015 at most stations.

3.2. Spatial distribution of ET_0 and climatic driving factors

Fig.5 shows the spatial distribution of trends in annual ET_0 and other climatic driving factors at the 22 meteorological stations during the periods from 1961 to 1991 and 1992 to 2015. Annual ET_0 showed decreasing trends at 21 of the 22 stations, Tanggu station being the exception, from 1961 to 1991, and these decreasing trends were significant ($p < 0.05$) at 13 stations. During the 1992–2015, ET_0 showed an increasing trend at 9 stations in the middle northern region, and these increasing trends were significant ($p < 0.05$) at 6 out of the 9 stations. The decreasing trend continued in the south, but was weaker than that before 1991 (Fig. 5a). The spatial change trends in wind speed resemble those of ET_0 (Fig. 5e). Decreasing trends in *SD* were identified in most regions, and only two showed non-significant increasing trends before and after 1991 (Fig. 5d). On the contrary, T_{mean} increased across the entire area during 1961–1990, but displayed a weakening trend after 1991, when T_{mean} began to decrease, especially in the central and northern regions.(Fig. 5b). Comparing the data before and after 1991, changes in *RH* show an uneven distribution, from increasing to decreasing at some stations, and from decreasing to increasing at others. Decreasing trends in *RH* in the southern part of Hebei Province and close to the Bohai Bay area have become significant over the last 24 years (Fig. 5c)

3.3. Relations between ET_0 and other climatic factors

Eq. (1) show that ET_0 is a function of T_{mean}, *RH, SD* and U_2U_2. As ET_0 is affected by multiple meteorological factors, and these factors may have mutual influences, the partial correlation method may be appropriate to identify any the 'real' correlation between ET_0 and a specific factor by eliminating the influences of all other factors (Gao et al., 2006). The partial correlation coefficients between ET_0 and other meteorological factors during the different periods are provided in Table 3.

These results show that ET_0 is positively correlated to mean air temperature, sunshine duration, and wind speed, and negatively correlated to relative humidity (Table 3). It is consistent with our common sense that increased temperature, wind speed, and sunshine duration will lead to an increase in ET_0, but that greater relative humidity will cause a decrease in ET_0. During 1961–1991, the wind speed exhibited the highest correlation with ET_0. The degree of correlation between ET_0 and other meteorological factors during this period decrease in the order: U_2, *RH*, T_{mean}, and *SD*, with correlation coefficients of 0.964, −0.935, 0.854, and 0.767, respectively, which are significant at the 1% level. After 1991, a strong correlation was found only between ET_0 and T_{mean}, with a correlation coefficient of 0.622 ($p < 0.01$). Correlation coefficients between ET_0 and other climatic factors were not significant, during the 1991–2015 interval.

3.4. Dominant factors of ET_0

In order to identify the rank of the meteorological factors affecting ET_0, the combined influences of the meteorological variables on ET_0 were also investigated. The multiple linear regression method is used to evaluate the relationship between ET_0 and all meteorological variables, and is applied to analyze the relative contribution of the meteorological factors to ET_0. The multiple linear regression is analyzed using data from the 1961–1991 and 1992–2015 periods, and the relative contribution of each factor was calculated using Eqs. (15) and (16); results are presented in Table 4.

Taking the period from 1961 to 1991, U_2 was found to be the primary factor and *RH* was the second most important factor influencing ET_0, followed by T_{mean} and *SD*. The increasing T_{mean} and decreasing *RH* led to an increase in ET_0, with relative contributions of 18.3% and 18.9%, respectively. But the decreases in U_2 and *SD* should have led to a decrease in ET_0, with relative contributions of 52.5% and 10.2%, respectively. The reductions in U_2 and *SD* offset the impacts of increasing T_{mean} and decreasing *RH*. The combined influences of the four climate factors eventually result in a decrease in ET_0. From 1992 to 2015, however, the increase in T_{mean} was the most dominant factor contributing to the increase in ET_0 with a relative contribution of 47.4%. In addition, the increasing U_2 and decreasing *RH* also exacerbated the increase of ET_0 to some extent, with relative contributions of 22.2% and 16.6%, respectively. The decline of *SD* should have led to decrease in ET_0 with its relative contribution of 13.8%. Obviously, changes in the climate variables (other than *SD*) have led to an increase in ET_0 since 1992.

Previous studies using contribution analysis methods emphasized that the multiple regression analysis method could not calculate the actual contribution rate of each climatic factor (Wang et al., 2016). The actual contribution rate is not only related to the importance of the climatic factors, but also to the specific variation amplitude of each factor (Liu et al., 2012; Zhang et al., 2013). Previous studies support finding that decreasing wind speed, sunshine duration, and solar radiation cause decreasing ET_0 (Shan et al., 2015; Xu et al., 2015). Wang et al. (2011) found that sunshine duration and wind speed were the major contributing variables for the decreasing trends in reference evapotranspiration in the Haihe River basin. However, Tang et al. (2011) concluded that ET_0 is most sensitive to air temperature and wind speed in the same region, consistent with the results presented for the 1992–2015 period in our study. The results partly differ in the same region mainly due to the different contribution analysis methods for ET_0 and the different research periods.

Either the net solar radiation or the sunshine duration was analyzed as the factor for the climatic contribution of the evapotranspiration in the literatures (Cong et al., 2009; Han et al., 2012; Shan et al., 2015; Breña-Naranjo et al., 2017;). In this paper, we choose the directly observed sunshine duration as one of the climatic indicators. There is a

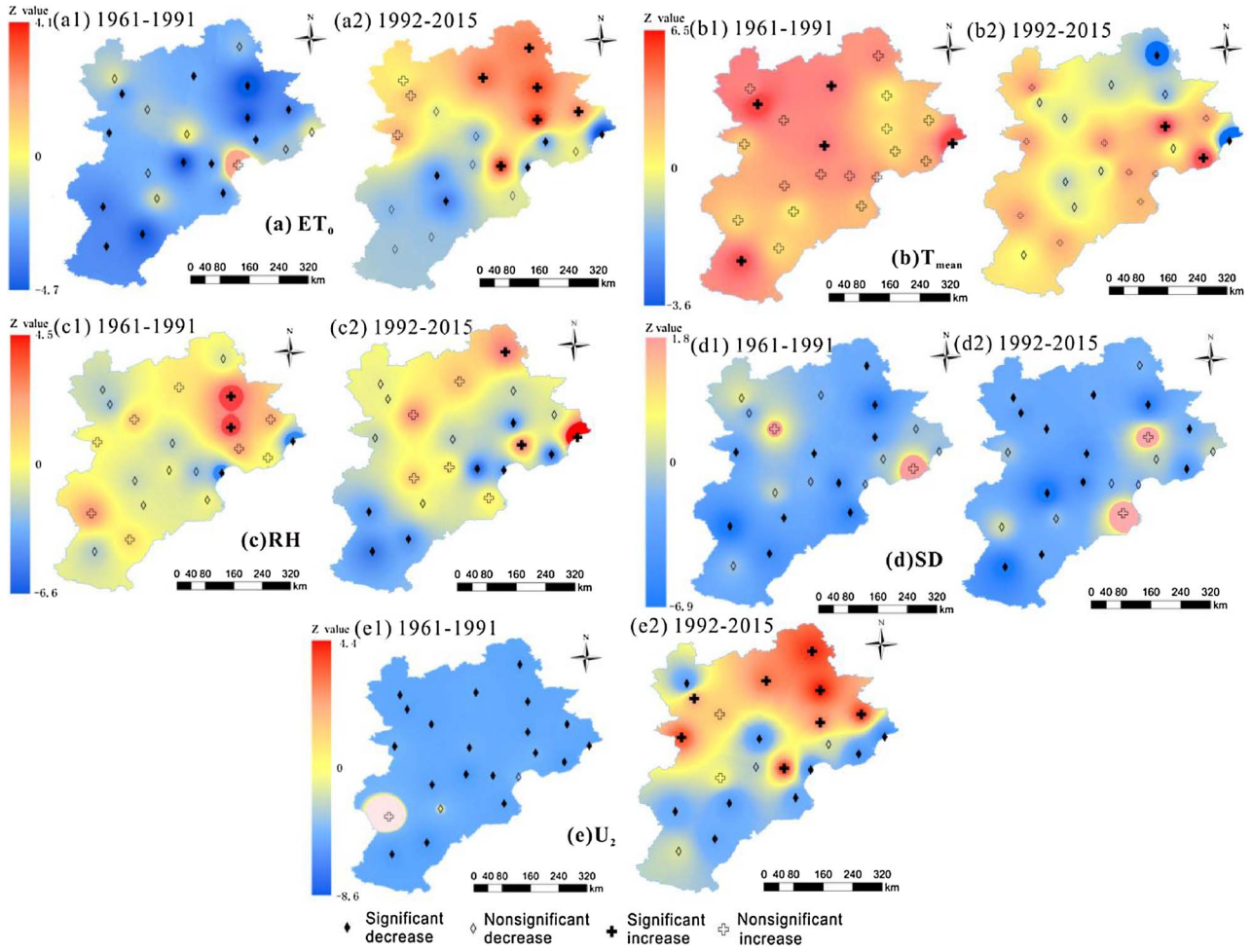

Fig. 5. Z value of MK trends from two periods (a)ET_0; (b) T_{mean}; (c) *RH*; (d) *SD*; (e) U_2; The legend indicates the Z value of the indicated meteorological factor. The range of Z values for three different periods are represented by the same legend. Deeper colors represent more significant changes. Red colors represent upward trends, and blue colors represent downward trends. (For interpretation of the references to colour in this figure legend, the reader is referred to the web version of this article.)

Table 3
Partial correlation coefficients between ET_0 and other meteorological factors.

Period	Mean air temperature (T_{mean})	Relative humidity (RH)	Sunshine duration (SD)	Wind speed (U_2)
1961–1991	0.854**	−0.935**	0.767**	0.964**
1992–2015	0.622**	−0.267	0.263	0.289

** Significance level of 0.01 ($p < 0.01$).

positive correlation between SD and net radiation from Eqs. (2)–(5). There are some underlying assumptions in the conversion of SD and radiation, the albedo coefficient α, the Angstrom coefficients a_s and b_s are assumed to be a fixed value when calculating net radiation. The critical assumptions do not actually reflect complex atmospheric conditions of the regional environmental characteristics, such as changes in atmospheric transmittance, humidity, aerosols and sun angles. Although there are some potential biases and uncertainties in the conversion of *SD* and radiation (Wu et al., 2017), the correlation coefficient between the calculated solar radiation and the observed solar radiation at solar radiation sites was larger than 0.9 in the Haihe River Basin (Liu et al., 2010). The *SD* can be used as an index to analyze the ET_o attribution when the solar radiation data is not available directly.

Human activities inevitably impact ET_0, through the impact on meteorological factors. Zhao et al. (2014) found that the trends of ET_0 in regions with the most intense human activities were most pronounced in the Hai River basin. Liu et al. (2010) demonstrated that the

Table 4
Correlation coefficients and relative contributions rate to ET_0 of the climatic driving factors.

Period	meteorological factors	Standardized Coefficients	Relative Contributions	Influence degree sort (greatest to least)
1961-1991	Relative humidity(RH)	−0.443	18.9%	U_2, RH, T_{mean}, SD
	Mean air temperature (T_{mean})	0.429	18.3%	
	Wind speed (U_2)	1.228	52.5%	
	Sunshine duration (SD)	0.239	10.2%	
1992-2015	Relative humidity(RH)	−0.289	16.6%	T_{mean}, U_2, RH, SD
	Mean air temperature (T_{mean})	0.826	47.4%	
	Wind speed (U_2)	0.387	22.2%	
	Sunshine duration (SD)	0.241	13.8%	

increase in aerosols caused by human activities was an important cause of reduction in solar radiation. Qian et al. (2006) speculated that the increased air pollution may lead to less solar radiation reaching the surface.In addition, urbanization has changed the surroundings of meteorological stations, affecting, for example, trends of mean wind speed. Decreasing trends of mean wind speed at urban stations in China are greater than those at rural stations during the period from 1956 to 2004 (Jiang et al., 2009). Changes in climatic factors resulting from human activities must eventually lead to changes in ET_0. Because the Jing-Jin-Ji region is one of China's most rapidly developing areas, the effect of human activities on ET_0 needs to be researched further, specifically to changes in land use and cover.

4. Conclusions

The spatial and temporal changes in ET_0 and its climatic driving factors in the Jing-Jin-Ji region were investigated using 1961–2015 data from the 22 national meteorological stations in the area. The main conclusions of this study are :

- A change point in the annual ET_0 series was detected around the year 1991 with Cramer's test; annual ET_0 decreased significantly at a rate of −20.95 mm/decade from 1961 to 1991, while annual ET_0 increased significantly at a rate of 7.40 mm/decade from 1992 to 2015. Before 1991, T_{mean} increased significantly and *RH* decreased insignificantly while U_2 and *SD* decreased significantly. After 1991, T_{mean} increased insignificantly and U_2 increased significantly while *RH* and *SD* decreased significantly. Spatially, the results demonstrated evaporation paradox conditions at all station except Tanggu before 1991, however, 54% of these stations did not show this phenomenon after 1991.
- ET_0 has significant positive correlations with T_{mean}, *SD* and U_2, but is negatively correlated to *RH*. From 1961 to 1991, U_2 was the dominant factor contributing to ET_0. The increasing T_{mean} and decreasing *RH* had a positive effect on annual ET_0, but this impact was offset by reductions in U_2 and *SD*. From 1992 to 2015, T_{mean} was found to be the most dominant factor leading to an increase in ET_0. The increasing T_{mean}, increasing U_2, and decreasing *RH* all led to an increase in ET_0 which offset the effect of decreasing *SD*.

The results of this study are significant for understanding the hydrological cycle and improving agricultural water management in the Jing-Jin-Ji region, and the impacts of ET_0 and climate factors on crop water requirements and agriculture irrigation management will be studied further and greater depth in our future work.

Acknowledgements

This research was supported by funds from the National key Research and Development Program of China (Grant No. 2016YFC0401407), the National Natural Science Foundation of China (Grant No. 51379216), the International Science & Technology Cooperation Program of China (Grant No. 2016YFE0102400), and the Open Research Fund of State Key Laboratory of Simulation and Regulation of Water Cycle in River Basin (China Institute of Water Resources and Hydropower Research) (Grant No. IWHR-SKL-201706)

References

Allen, R.G., Pereira, L.S., Raes, D., Smith, M., 1998. Crop Evapotranspiration: Guidelines for Computing Crop Water Requirements. FAO Irrigation and Drainage Paper No. 56. FAO, Rome, Italy.

Breña-Naranjo, J.A., Laverde-Barajas, M.Á., Pedrozo-Acuña, A., 2017. Changes in pan evaporation in Mexico from 1961 to 2010. Int. J. Climatol. 37 (1), 204–213.

Christensen, N.S., Wood, A.W., Voisin, N., Lettenmaier, D.P., Palmer, R.N., 2004. The effects of climate change on the hydrology and water resources of the Colorado River basin. Clim. Change 62, 337–363.

Cong, Z.T., Yang, D.W., Ni, G.H., 2009. Does evaporation paradox exist in China? Hydrol. Earth Syst. Sci. 13 (3), 357–366.

Dong, J., Zhuang, D.F., Xu, X.L., Ying, L., 2008. Integrated evaluation of urban development suitability based on remote sensing and GIS techniques–a case study in Jingjinji area, China. Sensors 8, 5975–5986.

Fan, L.L., Wang, H.R., Luo, W.B., Li, Y.L., Yuan, N.N., 2016. A study of flood and drought spatial characteristics and its impact on agricultural water in Jing-Jin-Ji region. China Rural Water Hydropower 8, 150–155 (in Chinese).

Feng, Z.M., Liu, D.W., 2006. A study on water resources carrying capacity in Jingjinji region. J. Nat. Resour. 21 (5), 689–699 (in Chinese).

Gao, G., Chen, D.L., Ren, G.Y., Chen, Y., Liao, Y.M., 2006. Spatial and temporal variations and controlling factors of potential evapotranspiration in China: 1956–2000. J. Geogr. Sci. 16 (1), 3–12.

Gao, X.R., Zhao, Q., Zhao, X.N., Wu, P.T., Pan, W.X., Gao, X.D., Sun, M., 2017. Temporal and spatial evolution of the standardized precipitation evapotranspiration index (SPEI) in the Loess Plateau under climate change from 2001 to 2050. Sci. Total Environ. 595, 191–200.

Han, S.J., Xu, D., Wang, S.L., 2012. Decreasing potential evaporation trends in China from 1956 to 2005: accelerated in regions with significant agricultural influence? Agric. For. Meteorol. 154–155, 44–56.

Huang, Y.H., Wang, J.H., Jiang, D., Zhou, K., Ding, X.Y., Fu, J.Y., 2014. Surface water deficiency zoning of China based on surface water deficit index (SWDI). Water Resour. 41 (4), 372–378.

Jiang, Y., Luo, Y., Zhao, Z.C., Tao, S.W., 2009. Changes in wind speed over China during 1956–2004. Theor. Appl. Climatol. 99, 421–430.

King, D.A., Bachelet, D.M., Symstad, A.J., Ferschweiler, K., Hobbins, M., 2015. Estimation of potential evapotranspiration from extraterrestrial radiation, air temperature and humidity to assess future climate change effects on the vegetation of the Northern Great Plains, USA. Ecol. Model. 297, 86–97.

Li, C., Wu, P.T., Li, X.L., Zhou, T.W., Sun, S.K., Wang, Y.B., Luan, X.B., Yu, X., 2017. Spatial and temporal evolution of climatic factors and its impacts on potential evapotranspiration in Loess Plateau of Northern Shaanxi, China. Sci. Total Environ. 589, 165–172.

Li, Z.X., Feng, Q., Liu, W., Wang, T.T., Gao, Y., Wang, Y.M., Cheng, A.F., Li, J.G., Liu, L., 2014. Spatial and temporal trend of potential evapotranspiration and related driving forces in Southwestern China, during 1961–2009. Quart. Int. 336, 127–144.

Lin, P.F., He, Z.B., Du, J., Chen, L.F., Zhu, X., Li, J., 2017. Recent changes in daily climate extremes in an arid mountain region, a case study in northwestern China's Qilian Mountains. Sci. Rep. 7 (2245), 1–15.

Liu, C.M., Liu, X.M., Zheng, H.X., Zeng, Y., 2010. Change of the solar radiation and its causes in the Haihe River basin and surrounding areas. J. Geogr. Sci. 20 (4), 569–580.

Liu, H.J., Li, Y., Josef, T., Zhang, R.H., Huang, G.H., 2014. Quantitative estimation of climate change effects on potential evapotranspiration in Beijing during 1951–2010. J. Geogr. Sci. 24 (1), 93–112.

Liu, X.M., Zhang, D., 2013. Trend analysis of reference evapotranspiration in Northwest China: the roles of changing wind speed and surface air temperature. Hydro Process 27 (26), 3941–3948.

Liu, X.M., Zhang, D., Luo, Y.Z., Liu, C.M., 2012. Spatial and temporal changes in aridity index in northwest China: 1960–2010. Theor. Appl. Climatol. 112, 307–316.

Ma, X.N., Zhang, M.J., Li, Y.J., Wang, S.J., Ma, Q., Liu, W.L., 2012. Decreasing potential evapotranspiration in the Huanghe River Watershed in climate warming during 1960–2010. J. Geogr. Sci. 22 (6), 977–988.

Moonen, A.C., Ercoli, L., Mariotti, M., Masoni, A., 2002. Climate change in Italy indicated by agrometeorological indices over 122 years. Agric. For. Meteorol. 111, 13–27.

Nam, W.H., Hong, E.M., Choi, J.Y., 2015. Has climate change already affected the spatial distribution and temporal trends of reference evapotranspiration in South Korea? Agric. Water Manage. 150, 129–138.

Ning, T.T., Li, Z., Liu, W.Z., Han, X.Y., 2016. Evolution of potential evapotranspiration in the northern Loess Plateau of China: recent trends and climatic drivers. Int. J. Climatol. 36, 4019–4028.

Peterson, T.C., Golubev, V.S., Groisman, P.Y., 1995. Evaporation losing its strength. Nature 377 (6551), 687–688.

Qian, Y., Kaiser, D.P., Leung, L.R., Xu, M., 2006. More frequent cloud-free sky and less surface solar radiation in China from 1955 to 2000. Geophy. Res. Lett. 33, 1–4.

Roderick, M.L., Farquhar, G.D., 2002. The cause of decreased pan evaporation over the past 50 years. Science 298, 1410–1411.

Roderick, M.L., Farquhar, G.D., 2005. Changes in New Zealand pan evaporation since the 1970s. Int. J. Climatol. 25, 2031–2039.

Shan, N., Shi, Z.J., Yang, X.H., Gao, J.X., Cai, D.W., 2015. Spatiotemporal trends of reference evapotranspiration and its driving factors in the Beijing–Tianjin Sand source control project region, China. Agric. For. Meteorol. 200, 322–333.

Tabari, H., Marofi, S., 2010. Changes of pan evaporation in the west of Iran. Water Resour. Manage. 25, 97–111.

Tang, B., Tong, L., Kang, S.Z., Zhang, L., 2011. Impacts of climate variability on reference evapotranspiration over 58 years in the Haihe river basin of North China. Agric. Water Manage. 98, 1660–1670.

Tao, X.E., Chen, H., Xu, C.Y., Hou, Y.K., Jie, M.X., 2015. Analysis and prediction of reference evapotranspiration with climate change in Xiangjiang River basin, China. Water Sci. Eng. 8 (4), 273–281.

Walther, G.R., Post, E., Convey, P., Menzel, A., Parmesan, C., Beebee, T.J.C., Fromentin, J.M., Ove, H.G., Bairlein, F., 2002. Ecological responses to recent climate change. Nature 416, 389–395.

Wang, Q.M., Wang, J.H., Zhao, Y., Li, H.H., Zhai, J.Q., Yu, Z.B., Zhang, S.Y., 2016. Reference evapotranspiration trends from 1980 to 2012 and their attribution to meteorological drivers in the three-river source region, China. Int. J. Climatol. 36, 3759–3769.

Wang, W.G., Peng, S.Z., Yang, T., Shao, Q.X., Xu, J.Z., Xing, W.Q., 2011. Spatial and temporal characteristics of reference evapotranspiration trends in the Haihe river basin, China. J. Hydrol. Eng. 16 (3), 239–252.
Wu, B.F., Liu, S.F., Zhu, W.W., Yan, N.N., Xing, Q., Tan, S., 2017. An improved approach for estimating daily net radiation over the Heihe river basin. Sensors 17 (1), 86.
Xia, J., Heung, W., Wai, C.Ip., 2003. Water problems and sustainability in North China. Water Resources Systems-Water Availability and Global Changes. IAHS, Sapporo, pp. 12–22.
Xu, L.H., Shi, Z.J., Wang, Y.H., Zhang, S.L., Chu, X.Z., Yu, P.T., Xiong, W., Zuo, H.J., 2015. Spatiotemporal variation and driving forces of reference evapotranspiration in Jing river basin, northwest China. Hydrol Process 29, 4846–4862.
Xu, Z.C., Tang, Y., Connor, T., Li, D.P., Li, Y.K., Liu, J.G., 2017. Climate variability and trends at a national scale. Sci. Rep. 7 (3258), 1–10.
Zhang, D., Liu, X.M., Hong, H.Y., 2013. Assessing the effect of climate change on reference evapotranspiration in China. Stoch. Environ. Res. Risk A 27, 1871–1881.
Zhang, K.X., Pan, S.M., Zhang, W., Xu, Y.H., Cao, L.G., Hao, Y.P., Wang, Y., 2015. Influence of climate change on reference evapotranspiration and aridity index and their temporal-spatial variations in the Yellow river basin, China, from 1961 to 2012. Quart. Int. 380–381, 75–82.
Zhang, Y.Q., Liu, C.M., Tang, Y.H., Yang, Y.H., 2007. Trends in pan evaporation and reference and actual evapotranspiration across the Tibetan Plateau. J. Geophys. Res. 112, 1–12.
Zhao, L.L., Xia, J., Sobkowiak, L., Li, Z.L., 2014. Climatic characteristics of reference evapotranspiration in the Hai river basin and their attribution. Water 6, 1482–1499.
Zhu, G.F., He, Y.Q., Pu, T., Wang, X.F., Jia, W.X., Li, Z.X., Xin, H.J., 2012. Spatial distribution and temporal trends in potential evapotranspiration over Hengduan Mountains region from 1960 to 2009. J. Geogr. Sci. 22 (1), 71–85.
Zhu, X.F., Zhao, A.Z., Li, Y.Z., Liu, X.F., 2015. Agricultural irrigation requirements under future climate scenarios in China, J. Arid Land 7 (2), 224–237.